



## Measurements of hydrogen sulfide (H<sub>2</sub>S) using PTR-MS: calibration, humidity dependence, inter-comparison and results from field studies in an oil and gas production region

R. Li<sup>1,2,3</sup>, C. Warneke<sup>1,2</sup>, M. Graus<sup>1,2,\*</sup>, R. Field<sup>4</sup>, F. Geiger<sup>5</sup>, P. R. Veres<sup>1,2</sup>, J. Soltis<sup>4</sup>, S.-M. Li<sup>6</sup>, S. M. Murphy<sup>4</sup>, C. Sweeney<sup>7</sup>, G. Pétron<sup>7</sup>, J. M. Roberts<sup>1</sup>, and J. de Gouw<sup>1,2</sup>

<sup>1</sup>Chemical Sciences Division, Earth System Research Laboratory, National Oceanic and Atmospheric Administration, Boulder, CO 80305, USA

<sup>2</sup>Cooperative Institute for Research in Environmental Sciences, University of Colorado, Boulder, CO 80309, USA

<sup>3</sup>Department of Atmospheric & Oceanic Sciences, University of Colorado, Boulder, CO 80309, USA

<sup>4</sup>Department of Atmospheric Science, University of Wyoming, Laramie, WY 82071, USA

<sup>5</sup>Karlsruhe Institute of Technology, IMK-ASF, Karlsruhe, Germany

<sup>6</sup>Air Quality Research Division, Science and Technology Branch, Environment Canada, 4905 Dufferin Street, Toronto, Ontario, M3H 5T4, Canada

<sup>7</sup>Global Monitoring Division, Earth System Research Laboratory, National Oceanic and Atmospheric Administration, Boulder, CO 80305, USA

\* now at: Institute of Meteorology and Geophysics, Innsbruck University, Austria

Correspondence to: R. Li (rui.li@noaa.gov)

Received: 9 May 2014 – Published in Atmos. Meas. Tech. Discuss.: 20 June 2014

Revised: 11 September 2014 – Accepted: 18 September 2014 – Published: 29 October 2014

**Abstract.** Natural gas production is associated with emissions of several trace gases, some of them classified as air toxics. While volatile organic compounds (VOCs) have received much attention, hydrogen sulfide (H<sub>2</sub>S) can also be of concern due to the known health impacts of exposure to this hazardous air pollutant. Here, we present quantitative, fast time-response measurements of H<sub>2</sub>S using proton-transfer-reaction mass-spectrometry (PTR-MS) instruments. An ultra-light-weight PTR-MS (ULW-PTR-MS) in a mobile laboratory was operated for measurements of VOCs and H<sub>2</sub>S in a gas and oil field during the Uintah Basin Winter Ozone Study (UBWOS) 2012 campaign. Measurements of VOCs and H<sub>2</sub>S by a PTR-MS were also made at the Horse Pool ground site in the Uintah Basin during UBWOS 2013. The H<sub>2</sub>S measurement by PTR-MS is strongly humidity dependent because the proton affinity of H<sub>2</sub>S is only slightly higher than that of water. The H<sub>2</sub>S sensitivity of PTR-MS ranged between 0.6–1.4 ncps ppbv<sup>-1</sup> during UBWOS 2013. We compare the humidity dependence determined in the laboratory with in-field calibrations and determine the H<sub>2</sub>S mixing ra-

tios for the mobile and ground measurements. The PTR-MS measurements at Horse Pool are evaluated by comparison with simultaneous H<sub>2</sub>S measurements using a PTR time-of-flight MS (PTR-ToF-MS) and a Picarro cavity ring down spectroscopy (CRDS) instrument for H<sub>2</sub>S/CH<sub>4</sub>. On average 0.6 ± 0.3 ppbv H<sub>2</sub>S was present at Horse Pool during UBWOS 2013. The correlation between H<sub>2</sub>S and methane enhancements suggests that the source of H<sub>2</sub>S is associated with oil and gas extraction in the basin. Significant H<sub>2</sub>S mixing ratios of up to 9 ppmv downwind of storage tanks were observed during the mobile measurements. This study suggests that H<sub>2</sub>S emissions associated with oil and gas production can lead to short-term high levels close to point sources, and elevated background levels away from those sources. In addition, our work has demonstrated that PTR-MS can make reliable measurements of H<sub>2</sub>S at levels below 1 ppbv.

## 1 Introduction

Hydrogen sulfide (H<sub>2</sub>S) is a flammable gas that is highly toxic at low concentrations; e.g., at 10–20 ppmv H<sub>2</sub>S starts causing eye irritation and at levels above 150 ppmv it is life threatening. The primary emission sources of H<sub>2</sub>S to the atmosphere include volcanic eruptions, natural decomposition of sulfates and sulfur-containing organic compounds by anaerobic bacteria, and anthropogenic release from industrial processes. H<sub>2</sub>S is also emitted from coal pits, landfills, livestock manure, thermal or polluted waters and septic systems (Environmental Protection Agency et al., 1993). Hydrogen sulfide is a major impurity in natural gas that needs to be removed prior to use. In oil and gas operations, H<sub>2</sub>S can be released routinely or accidentally at wellheads, piping, separation and storage tanks (Environmental Protection Agency et al., 1993; Tarver and Dasgupta, 1997). Previous H<sub>2</sub>S studies in oil fields indicated that hydrogen sulfide was the dominant reduced sulfur gas in all the sampled oil producing locations (Tarver and Dasgupta, 1997).

One study showed that the mixing ratios of H<sub>2</sub>S in ambient air range from 0.02–0.07 ppbv in undeveloped rural areas to 0.11–0.33 ppbv in urban areas (Chou et al., 2006). Ambient air quality guidelines for H<sub>2</sub>S have been developed in many states, which range from 14 to 160 ppbv per 24 h averaging time. H<sub>2</sub>S is regulated under a number of US statutes, including the Comprehensive Environmental Response, Compensation, and Liability Act (CERCLA), the Emergency Planning and Community Right-to-Know Act (EPCRA), and the Prevention of Significant Deterioration (PSD) program of the EPA for regulation of new oil and gas well sources (Chou et al., 2006; DUBYK et al., 2002). The familiar “rotten egg” odor of H<sub>2</sub>S becomes detectable by humans at concentrations of 3–20 ppbv. However, higher concentrations of H<sub>2</sub>S in the 150–250 ppmv range can cause olfactory paralysis. At these concentrations, the olfactory sense may be lost and exposed persons may be unaware of the presence of the toxic gas. Thus, odor cannot be relied upon as a warning sign of possible exposure to H<sub>2</sub>S (Environmental Protection Agency et al., 1993). Little public data exist to determine actual levels of H<sub>2</sub>S near oil and gas production sites. After an incident known as the Lodgepole blowout, maximum hourly H<sub>2</sub>S concentrations as high as 15 ppmv were measured at different locations within a 20 km radius around Alberta, Canada (Layfon and Cederwall, 1987; Skrtic, 2006). A geological survey from the Department of Environment Quality of Michigan showed that over 12 % of producing oil wells in Michigan had oil H<sub>2</sub>S contents exceeding 300 ppm by mass (Office of Geological Survey, 2013). In the atmosphere, H<sub>2</sub>S has a lifetime of a few hours during the day due to reactions with OH. It has also been suggested that H<sub>2</sub>S can be oxidized to form sulfate on suspended alkaline dust (Tarver and Dasgupta, 1997).

Various techniques have been used for H<sub>2</sub>S measurements. Gas chromatography with flame photometric detection (GC-

FPD) was used before the 1990s (Stuedler and Kijowski, 1984). These instruments have relatively poor detection limits (> 1 ppm) and are insufficient to detect H<sub>2</sub>S at ambient levels (Benner and Stedman, 1990). Chemiluminescence instruments based on reaction with ClO<sub>2</sub> (Spurlin and Yeung, 1982), O<sub>3</sub> (Kelly et al., 1983) and excited SO (Benner and Stedman, 1989) have a detection limit of 130 pptv for H<sub>2</sub>S, but there exist potential interferences from other hydrocarbons in environments like oil fields. Other commonly used instruments are based on cavity ring-down spectroscopy (CRDS) and gas chromatography coupled with isotope dilution mass spectrometry (Bandy et al., 1985) and sulfur chemiluminescence detection (GC-SCD) (Khan et al., 2012). Existing measurements also use catalytic conversion of H<sub>2</sub>S into sulfur dioxide (SO<sub>2</sub>) and detection of SO<sub>2</sub> by pulsed fluorescence (Heber et al., 2010; Z. Liu et al., 2011). This method has a limited sensitivity (detection limit of 6 ppbv in 10 s) and can have interferences from the presence of transient concentrations of SO<sub>2</sub> and other reduced sulfur compounds. Moreover, SO<sub>2</sub> detection by pulsed fluorescence is susceptible to interference by polycyclic hydrocarbons, which are also emitted from natural gas production operations (Heber et al., 2010; Z. Liu et al., 2011).

Recently, proton-transfer-reaction mass spectrometry (PTR-MS) has been used to detect H<sub>2</sub>S in agricultural and food studies (Liu et al., 2013; Feilberg et al., 2010; D. Liu et al., 2011; Saha et al., 2011), olfactometer characterization (Beauchamp et al., 2010), and other laboratory settings in spite of various analytical challenges (Feilberg et al., 2013). In this work, we characterized the humidity dependence of the instrument responses to H<sub>2</sub>S of PTR-MS, and explored its application for quantitative measurements of H<sub>2</sub>S in the air over an oil and gas field.

## 2 Experimental

The Uintah Basin in northeastern Utah (Fig. 1), a region with approximately 8000 gas wells and 2000 oil wells in operation, experienced high wintertime surface ozone concentrations in the winters 2009/2010 and 2010/2011 (Martin et al., 2011). Two field intensives, the Energy and Environment – Uintah Basin Winter Ozone Study (UBWOS), were conducted in the winters of 2012 (15 January–28 February) and 2013 (15 January–28 February). An extensive suite of research instruments were deployed by a large group of scientists from different institutions at a well pad (named Horse Pool, 40 143° N; 109 468° W; 1530 m elevation) located on the northern edge of the gas field, 20 miles south of Vernal, UT in both years. The NOAA Earth System Research Laboratory (ESRL) also surveyed the Uintah Basin with an instrumented van, called here the Mobile Laboratory, to document ambient levels of methane and ozone precursors downwind of various point sources. The main goals of this project were to quantify the emission of ozone precursors from the oil

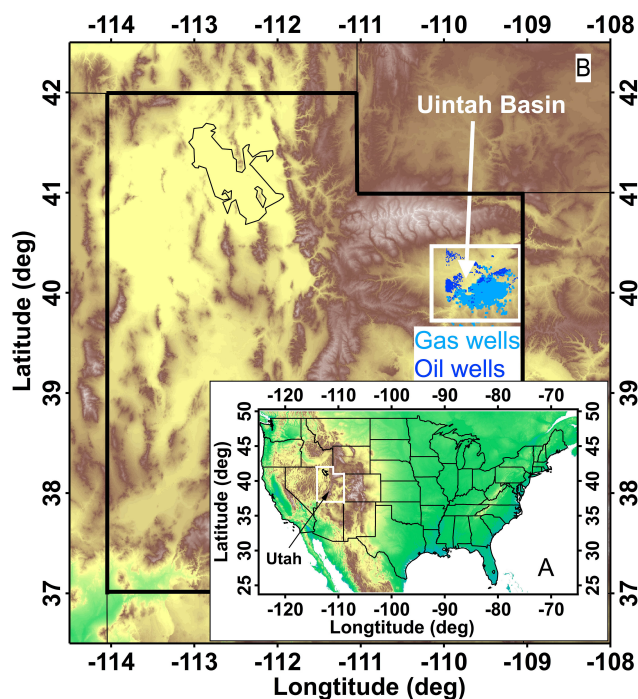


**Figure 1.** (a) The location of Utah in the overview map of United States. (b) The oil and gas wells in Uintah Basin, Utah.

and gas wells, and to understand the mechanisms of ozone formation in the basin in winter. The OH reactivity from H<sub>2</sub>S ( $\sim 0.1 \text{ s}^{-1}$ ) is a small fraction of the total OH reactivity ( $\sim 30 \text{ s}^{-1}$ ) observed in the basin, indicating that H<sub>2</sub>S is not an important precursor for ozone formation.

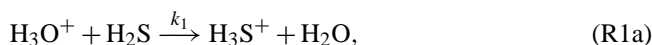
Measurements of H<sub>2</sub>S were made in the oil and gas field in the Uintah basin during the UBWOS 2012 and 2013, and during a laboratory study on H<sub>2</sub>S detection by PTR-MS after the 2013 UBWOS campaign (all measurements used here are summarized in Table 1). During UBWOS 2012 an ultra-light-weight proton-transfer-reaction mass spectrometer (ULW-PTR-MS,  $\sim 55 \text{ kg}$ ) (Warneke et al., 2014) was fielded together with a PTR-MS (de Gouw and Warneke, 2007). The ULW-PTR-MS was installed in the NOAA ESRL Mobile Laboratory for 2 weeks in February 2012 to make measurements downwind of point sources in the Uintah basin. In 2013, we further explored H<sub>2</sub>S detection by both PTR-MS and PTR time-of-flight mass spectrometry (PTR-ToF-MS) (Graus et al., 2010) at the Horse Pool ground site. Along with H<sub>2</sub>S, these instruments also simultaneously measured aromatics and oxygenated volatile organic compounds (VOCs). During these studies, regular calibrations on the PTR-MS instruments were performed using standard gas mixtures every other day. To evaluate the H<sub>2</sub>S measurements by PTR-MS we compare them with concurrent H<sub>2</sub>S measurements from a CRDS instrument (Model G2204, Picarro, Inc., Santa Clara, CA). A laboratory study was conducted to determine the hu-

midity dependence of the calibration factors of H<sub>2</sub>S for both the PTR-MS and PTR-ToF-MS.

## 2.1 H<sub>2</sub>S detection by PTR-MS

The application of PTR-MS for atmospheric measurements has been reviewed by de Gouw and Warneke (2007). Briefly, the detection principle is based on the proton-transfer reaction of the hydronium ion (H<sub>3</sub>O<sup>+</sup>) with H<sub>2</sub>S and VOCs that have a higher proton affinity (PA) than water. The proton-transfer reactions take place in a drift tube to minimize cluster ion formation and simplify the interpretation of mass spectra. The reagent and product ions are detected using a mass spectrometer, and the ion signal is proportional to the compound mixing ratio. A Platinum (Pt) catalyst is used to determine instrument backgrounds by removing VOCs and H<sub>2</sub>S in the sample air. The fragmentation from higher molecular weight species to form H<sub>3</sub>S<sup>+</sup> is not known to occur from compounds like CH<sub>3</sub>SH and CH<sub>3</sub>SCH<sub>3</sub>, which were very low at ambient conditions.

One significant challenge for H<sub>2</sub>S detection by PTR-MS is that H<sub>2</sub>S has only a slightly higher PA than water ( $691 \text{ kJ mol}^{-1}$  for H<sub>2</sub>O and  $705 \text{ kJ mol}^{-1}$  for H<sub>2</sub>S) (Hunter and Lias, 1998). Since the proton-transfer reaction (R1a) of H<sub>3</sub>O<sup>+</sup> with H<sub>2</sub>S is only slightly exothermic, the back reaction (R1b) is no longer negligible at typical settings in PTR-MS instruments (Feilberg et al., 2013):



The rate coefficients at 298 K are  $k_1 = 1.9 \times 10^{-9} \text{ cm}^3 \text{ molecule}^{-1} \text{ s}^{-1}$  and  $k_{-1} = 4.4 \times 10^{-12} \text{ cm}^3 \text{ molecule}^{-1} \text{ s}^{-1}$  (Tanaka et al., 1978). As a result, the H<sub>2</sub>S measurement by PTR-MS is affected by humidity and has a relatively low sensitivity. However, drying the sample flow to eliminate the humidity dependence of the sensitivity is not an option, because it will also result in losing many VOCs along with the water. It should also be noted that H<sub>2</sub>S proton transfer reaction with water cluster ions H<sub>3</sub>O<sup>+</sup> · H<sub>2</sub>O are not important due to a much slower reaction rate ( $< 10^{-12} \text{ cm}^3 \text{ molecule}^{-1} \text{ s}^{-1}$ ). No occurrence of competing channels by the water clustering reactions was observed in the measurement for H<sub>2</sub>S protonation under a wide range of humidity conditions (Tanaka et al., 1978). Therefore, the H<sub>2</sub>S reaction with water cluster is neglected in this work. The kinetics of the analogous reactions with formaldehyde (HCHO) has been studied in detail by Inomata et al. (2008); Vlasenko et al. (2010); Warneke et al. (2011b) and for HCN by Knighton et al. (2009). In a manner analogous to that work, the humidity dependent concentration of H<sub>3</sub>S<sup>+</sup> ion in the drift tube is given by the following:

**Table 1.** A list of studies with the time, instruments and purposes, from which the H<sub>2</sub>S data were used in this work.

Studies	Time	Instruments	Purposes
UBWOS 2012	Jan–Feb 2012	ULW-PTR-MS	Mobile measurements
UBWOS 2013	Jan–Feb 2013	PTR-MS PTR-ToF-MS Picarro	Ground measurements at Horse Pool
Laboratory	Mar 2013	PTR-MS PTR-ToF-MS	Calibrations Detection humidity dependence

$$[\text{H}_3\text{S}^+] = [\text{H}_3\text{O}^+] \frac{k_1 [\text{H}_2\text{S}] (1 - e^{-k_{-1}[\text{H}_2\text{O}]t})}{k_{-1} [\text{H}_2\text{O}]}, \quad (1)$$

where [H<sub>2</sub>S], [H<sub>2</sub>O] and [H<sub>3</sub>O<sup>+</sup>] are drift tube concentrations of H<sub>2</sub>S, water and hydronium ions, respectively, and  $t$  is the reaction time. Although the rate coefficient of the forward reaction (R1) is higher than of the reverse reaction (R1b) rate coefficient (i.e.,  $k_1 \gg k_{-1}$ ), the mixing ratio of water (typically 1 %) in the drift tube is much higher than H<sub>2</sub>S (< 10 ppbv) (i.e., [H<sub>2</sub>O]  $\gg$  [H<sub>2</sub>S]). The ratio ( $k_1 \times [\text{H}_2\text{S}] / (k_{-1} \times [\text{H}_2\text{O}])$ ) determines the final [H<sub>3</sub>S<sup>+</sup>] in the drift tube. It should be noted that the ion kinetic energy is elevated in the drift tube, and that the endothermic reactions (i.e., R1b) may be more important than based solely on the reaction enthalpy. As a result of back reaction (R1b), the production of protonated H<sub>2</sub>S is much less efficient than production of most protonated VOCs. In Eq. (1), [H<sub>3</sub>S<sup>+</sup>] is strongly dependent on the H<sub>2</sub>O concentration and the reaction time  $t$ . In Fig. 2, the [H<sub>3</sub>S<sup>+</sup>] in the drift tube calculated from Eq. (1) is plotted as a function of reaction time at various humidity conditions. The reaction time  $t$  is determined by the ion drift velocity, which is a function of the parameter  $E/N$ , where  $E$  is the electric field and  $N$  the number density of the gas in the drift tube (de Gouw and Warneke, 2007). The instrument settings used in this study are typical for the PTR-MS and are given in Table 2. These settings give a reaction time  $t$  of  $\sim 100 \mu\text{s}$ , which is not significantly different from other PTR instruments in Table 2. At higher water concentration, the reaction time is slightly lower due to a higher fraction of water clusters, which have lower ion mobility (Warneke et al., 2001). Another small effect is that ion mobilities in general are slightly lower in air-water vapor mixtures than in pure air. But these effects are very small and have been neglected in this work. It is worth noting that the forward and backward reactions are not necessarily in equilibrium. From Fig. 2 it is clear that at low water concentration conditions, the residence time of H<sub>3</sub>S<sup>+</sup> ions in the drift tube is insufficient for backward reaction (R1b) to get into equilibrium with the forward reaction (R1) at typical instrument settings. More H<sub>3</sub>S<sup>+</sup> ions are produced at lower water concentrations.

During the UBWOS 2013 campaign, the PTR-MS deployed at Horse Pool routinely measured 32 masses corresponding to different VOCs. These VOCs were measured for 1 second each along with 6 primary and impurity ions, resulting in a 38 s duty cycle. Background measurements for all masses were conducted every 3 h 15 min for 153 s.

The methanol isotope with a natural abundance of 0.2 % <sup>18</sup>O isotope is detected as CH<sub>3</sub><sup>18</sup>OH • H<sup>+</sup> ( $m/z$  35.0377) and at the same mass on the PTR-MS as H<sub>3</sub>S<sup>+</sup> ( $m/z$  34.9950) at unity mass resolution. This causes interference in the H<sub>2</sub>S measurements by PTR-MS under conditions with high methanol concentrations, as was the case in the oil and gas field in Utah and needs to be corrected for.

At a mass resolving power ( $R_{\text{FWHM}}$ , defined as mass at the peak center divided by the peak's full width at half maximum) greater than 1200, the methanol isotope and H<sub>3</sub>S<sup>+</sup> peaks are readily resolved (Graus et al., 2010). The PTR-ToF-MS (PTR-ToF 8000, Ionicon Analytik, Innsbruck, Austria) used here has a mass resolution of  $> 3000$  and clearly separates the peaks of the two ions. Since the PTR-ToF-MS data do not require any methanol isotope correction, the H<sub>2</sub>S detection limit of the PTR-ToF ( $\sim 200$  pptv) can be expected to be better than that of the PTR-MS instrument. During the UBWOS 2013 campaign, the PTR-ToF-MS was operated at the conditions given in Table 2 and with an extraction frequency of 250 kHz. Average mass spectra up to  $m/z$  500 were collected every 10 s.

## 2.2 Other instruments

Two CRDS instruments (Picarro, Inc) for CH<sub>4</sub> and H<sub>2</sub>S measurements were deployed together with the PTR-MS instruments at Horse Pool in 2013. A CRDS G2204 with CH<sub>4</sub> and H<sub>2</sub>S channels (CH<sub>4</sub>/H<sub>2</sub>S) was deployed for the first 2 weeks of UBWOS 2013 only. The CH<sub>4</sub> data used in this study were a combination of measurements from both the CH<sub>4</sub>/H<sub>2</sub>S and CH<sub>4</sub>/CO<sub>2</sub> (Picarro Model G2301) instruments. A detailed study of CH<sub>4</sub> measurements by CRDS techniques has been given by Chen et al. (2010) and Karion et al. (2013). The CH<sub>4</sub>/H<sub>2</sub>S CRDS used in this study has a measurement range of 0–20 ppm H<sub>2</sub>S. The H<sub>2</sub>S measurement precision is 1 ppbv + 0.4 % for 5 min averaged data. H<sub>2</sub>S calibrations were done before and during the campaign. The calibration results showed a zero drift of 0.3 ppb H<sub>2</sub>S during the

**Table 2.** The instrument settings of PTR-MS and PTR-ToF that affect the humidity-dependent sensitivities.

	Water flow <sup>a</sup> (sccm)	Pressure <sup>b</sup> (mbar)	Voltage <sup>b</sup> (V)	Temperature <sup>b</sup> (C)	$E/N^c$ (Td)
PTR-MS	10.5	2.4	720	45	117
PTR-ToF-MS	5	2.2	600	60	112
ULW-PTR-MS	7.5	2.2	612	40	106

<sup>a</sup> The water flow in the ion source. <sup>b</sup> The parameters of drift tube settings.

<sup>c</sup> The  $E/N$  is expressed in unit of Townsend (1 Td = 10<sup>-17</sup> V cm<sup>2</sup>).

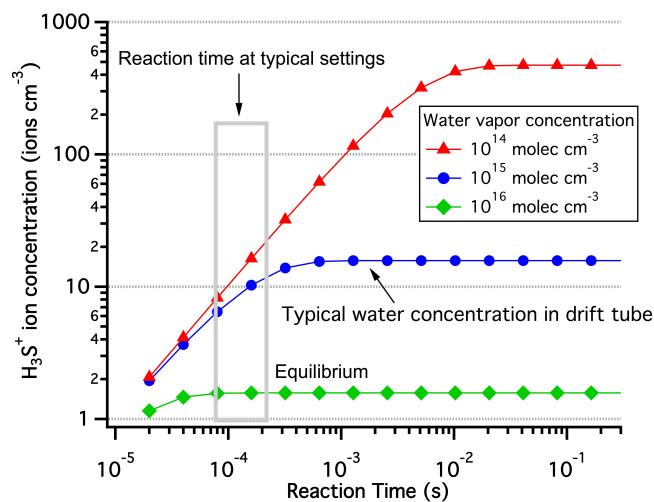


**Figure 2.** The concentration of H<sub>3</sub>S<sup>+</sup> ions as a function of reaction time in the drift tube at different humidities. The water vapor concentration in the drift tube ranges from  $0.5 \times 10^{15}$  to  $2 \times 10^{15}$  molec cm<sup>-3</sup> (equivalent to water vapor mixing ratio of 5.6–29.3 g kg<sup>-1</sup>).

campaign, which has been corrected for in the measurements. Little water interference was observed for the ambient H<sub>2</sub>S measurements in this study. The measurement interval is 5 s. The instrument records the signal at every 5 s as well as the averaged signal over the last 5 min cycle. The signals with averages of 5 min were used in this study.

### 3 Results and discussion

#### 3.1 Mobile laboratory measurement

The NOAA ESRL Mobile Laboratory performed 13 surveys in the oil and gas production areas in the Uintah basin in February 2012. The PTR-MS measurements included  $m/z$  35, i.e., the mass of protonated H<sub>2</sub>S, only on the surveys between 25–28 February. Here, the surveys on 27 and 28 February are presented (Fig. 3). Figure 3a shows the oil and gas well areas indicated by the white square in Fig. 1b and the drive tracks on both 27 and 28 February 2012, which were color- and size-coded by the raw signals at  $m/z$  35 (in

counts per second, cps). Figure 3b shows the time series of the  $m/z$  35 signals on 28 February. Most locations showed instrument signals below 50 cps. In contrast, signal enhancements of a factor of 3 were observed at a number of locations. The highest enhancement measured by the ULW-PTR-MS was observed during the drive on 27 February (Fig. 3c), in the area indicated by the white square in Fig. 3a. Figure 3d shows the time series of  $m/z$  35 signals for the drive shown on the map in Fig. 3c. Downwind of a condensate tank under service, the  $m/z$  35 signal was 40 000 cps, an enhancement of 3 orders of magnitude over ambient levels. Because the ULW-PTR-MS was not calibrated, the mobile laboratory H<sub>2</sub>S data is shown here in cps. Assuming that the sensitivity of the ULW-PTR-MS for H<sub>2</sub>S was similar with the PTR-MS and in the same range as for formaldehyde, for which calibration was performed on PTR-MS, these occasionally high count rates suggested that H<sub>2</sub>S was in the ppmv range. Such high mixing ratios were the motivation for the measurements described in the following. We will return to these data at the end of this paper.

#### 3.2 Laboratory calibration

Laboratory calibrations for H<sub>2</sub>S were performed after UB-WOS 2013 using the PTR-MS and PTR-ToF-MS at different humidities. Zero air was split using two mass flow controller (Tylan FC-260) channels, one of which passed air through a water bubbler filled with purified water ( $> 18.1$  MOhm cm<sup>-1</sup>) at 20 °C for humidification. Assuming near-saturation (23.3 mbar vapor pressure at an ambient pressure of 844 mbar and 20 °C) the water mixing ratio in the humidified channel was 2.84 % (17.7 g kg<sup>-1</sup>). The humidified zero air was mixed with dry zero air. This way the water vapor mixing ratio in the dilution gas was held at a constant level for individual calibration runs and could be changed rapidly from one setting to the next. The total flow rate of the humidified dilution gas stream was kept at approximately 500 sccm (cm<sup>3</sup> min<sup>-1</sup> at STP) and was measured volumetrically (Bios DryCal Definer 220) for each humidity setting. Up to 5 sccm (unit mass flow controller) of H<sub>2</sub>S from a calibration standard (10.08 ppmv  $\pm$  2 % H<sub>2</sub>S in N<sub>2</sub>; Scott-Marrin, Inc, Riverside, CA) was dynamically diluted with the humidified zero air and was sampled by both PTR instruments simultaneously. Calibrations with four

concentration levels (between 41 ppbv and 100 ppbv H<sub>2</sub>S) were performed at six humidity levels (water mixing ratios between 0 and 2.61 %, i.e., 0–16.3 g kg<sup>-1</sup>). In Fig. 4, the signals on  $m/z$  35 normalized to primary ion signals H<sub>3</sub>O<sup>+</sup> (in units of 10<sup>6</sup> counts s<sup>-1</sup>) from (a) PTR-MS and (b) PTR-ToF-MS are plotted versus the mixing ratio of H<sub>2</sub>S at different humidities. Calibrations at each individual humidity levels are fit separately by linear regression (lines in Fig. 4a and b, respectively). Observed slopes are the instrument sensitivities for different humidities and are plotted versus water vapor mixing ratio in Fig. 4c and d.

The PTR-MS had an average primary ion signal of 25 million cps and the PTR-ToF-MS had 8.8 million cps with duty cycle corrected (about 1.2 million cps actual counts) on average during UBWOS 2013. The differences in normalized sensitivities (in ncps ppbv<sup>-1</sup>) are likely due to the ion extraction and discrimination against smaller masses that are different between the quadrupole and time-of-flight mass spectrometers. As the absolute signal of the PTR-MS is higher, the sensitivity of the PTR-MS (in cps ppbv<sup>-1</sup>) can be higher than that of the PTR-ToF-MS.

As shown in Eq. (1), the H<sub>3</sub>S<sup>+</sup> ion signals are dependent on water concentration in the drift tube, which is governed by the water vapor concentration in the sample gas and by the amount of water vapor from the ion source leaking into the drift tube (Vlasenko et al., 2010; Warneke et al., 2011b). The resulting water vapor concentration in the drift tube is expressed as water vapor mass mixing ratio instead of water vapor number concentration, because mixing ratio is a conserved value as gas moves from ambient pressure into the drift tube at lower pressure. The calibration curves in Fig. 4 are color-coded with the water vapor mixing ratio in the sample gas. The sensitivity decreases when sample air humidity increases as the reverse proton transfer reaction (R1b) becomes more important with higher humidity.

Previous studies have demonstrated a reasonable agreement between the calibration measurements and the theoretical calculation using rate coefficients for proton transfer reactions for a number of VOCs with little humidity dependence (Warneke et al., 2003). In this study, the theoretical H<sub>2</sub>S sensitivities as a function of humidity are also investigated and compared to the laboratory calibration. An exponential fit derived from Eq. (1) is used to describe the humidity dependence of the H<sub>2</sub>S sensitivities. From the definition of the sensitivity, which is defined as the signal of RH<sup>+</sup> ions ( $I_{RH^+}$ ) obtained at a mixing ratio of 1 ppbv and normalized to a H<sub>3</sub>O<sup>+</sup> signal ( $I_{H_3O^+}^+$  of 10<sup>6</sup> cps, de Gouw and Warneke, 2007), the H<sub>2</sub>S sensitivity can be expressed as

$$\text{H}_2\text{S Sensitivity} = \frac{I_{\text{H}_3\text{S}^+}}{I_{\text{H}_3\text{O}^+}} \times \frac{10^6}{\text{H}_2\text{S}_{\text{VMR}}}, \quad (2)$$

where H<sub>2</sub>S<sub>VMR</sub> is the H<sub>2</sub>S volume mixing ratio (VMR) in ppbv

$$\text{H}_2\text{S}_{\text{VMR}} = \frac{[\text{H}_2\text{S}]}{N \times 10^{-9}}, \quad (3)$$

and  $N$  is the air number concentration in unit of molecule cm<sup>-3</sup> in the drift tube. H<sub>3</sub>S<sup>+</sup> and H<sub>3</sub>O<sup>+</sup> signals are related to their ion concentrations in the drift tube

$$\frac{I_{\text{H}_3\text{S}^+}}{I_{\text{H}_3\text{O}^+}} = \frac{[\text{H}_3\text{S}^+]}{[\text{H}_3\text{O}^+]} \times A. \quad (4)$$

$A$  is a factor that is determined by the ratio of transmission efficiencies for H<sub>3</sub>S<sup>+</sup> and H<sub>3</sub>O<sup>+</sup> ions, which varies in different PTR-MS instruments with different settings. Typically,  $A$  is relatively constant since the voltages to the detector and ion extraction are not changed frequently, and thus stable calibration factors can be obtained (de Gouw et al., 2003b). A previous study has shown  $A$  is mass dependent and increases with molecular weight (Warneke et al., 2011a). For different studies the instruments were usually tuned to optimize the measurement of the compounds of interest, and therefore, the  $A$  factor and sensitivities may be different. Using the calibration measurements in the field and the laboratory  $A$  is verified for compounds in the calibration standard and can be calculated for all other masses. In this study of H<sub>2</sub>S,  $A$  is assumed to be ~1.5 for PTR-MS based on the measured value of 1.6 for acetonitrile (mass 42) (de Gouw et al., 2003a). For PTR-ToF-MS,  $A$  is 1 for H<sub>3</sub>S<sup>+</sup> versus H<sub>3</sub>O<sup>+</sup> due to duty cycle correction on the ToF data (Müller et al., 2013). By substituting Eqs. (1), (3) and (4) into (2), the H<sub>2</sub>S sensitivity can be described as an exponential function of water:

$$\text{H}_2\text{S Sensitivity} = A \times 10^6 \times \frac{k_1 (1 - e^{-k_{-1}[\text{H}_2\text{O}]t})}{k_{-1}[\text{H}_2\text{O}]} \times N \times 10^{-9}. \quad (5)$$

The water concentration in the drift tube includes water vapor from the sampled air and from the ion source, which can be expressed as mass mixing ratio (H<sub>2</sub>O<sub>sample</sub> and H<sub>2</sub>O<sub>ion source</sub> in unit of g kg<sup>-1</sup>)

$$[\text{H}_2\text{O}] = (\text{H}_2\text{O}_{\text{sample}} + \text{H}_2\text{O}_{\text{ion source}}) \times \frac{M_{\text{air}}}{M_{\text{water}}} \times 10^{-3} \times N. \quad (6)$$

The molecular masses of air ( $M_{\text{air}}$ ) and water ( $M_{\text{water}}$ ) are 29 and 18 g mol<sup>-1</sup>. Using known coefficients  $k_1$  and  $k_{-1}$  from literature, reaction time  $t$ , air number concentration  $N$  and the sampled air humidity (H<sub>2</sub>O<sub>sample</sub>), the H<sub>2</sub>S sensitivity can be fit by Eq. (5) as a function of H<sub>2</sub>O<sub>sample</sub> for the data shown in Fig. 4c and d. The free parameters in the fit are the transmission ratio  $A$  and H<sub>2</sub>O<sub>ion source</sub>, which is the offset ( $x_{\text{offset}}$ ) on the  $x$  axis resulting from the additional water vapor from the ion source. The fit results give values for  $A$  of 0.3 ± 0.03

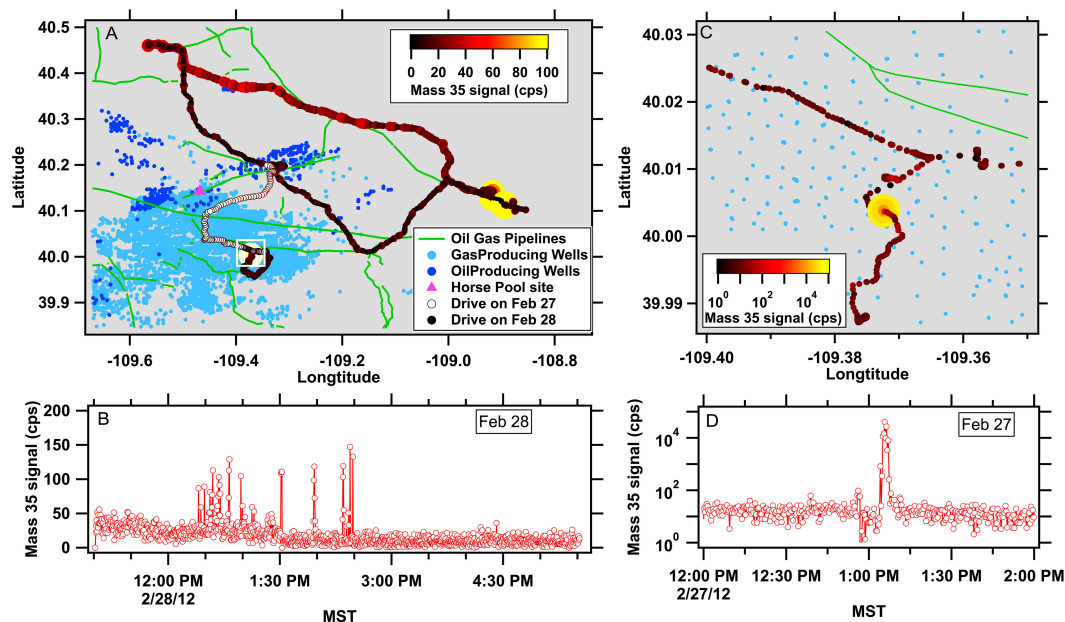


**Figure 3.** (a) Mobile laboratory tracks color- and size-coded with H<sub>2</sub>S signal at  $m/z$  35 by ULW-PTR-MS among the oil and gas wells in Uintah Basin during UBWOS 2012. (b) Time series of H<sub>2</sub>S signal at  $m/z$  35 on 28 February 2012 (solid points in A). (c) The area indicated by the white square in (a) for the drive on 27 February 2012. Note that the color scale of H<sub>2</sub>S signals is in log scale. (d) The time series of H<sub>2</sub>S measurements shown in (c). The peak H<sub>2</sub>S mixing ratio observed during this drive was determined to be 9 ppmv using the calibrations developed further below in this paper. Local time, i.e., Mountain Standard Time (MST) = UTC  $-7$  h is used in all the time-series plots.

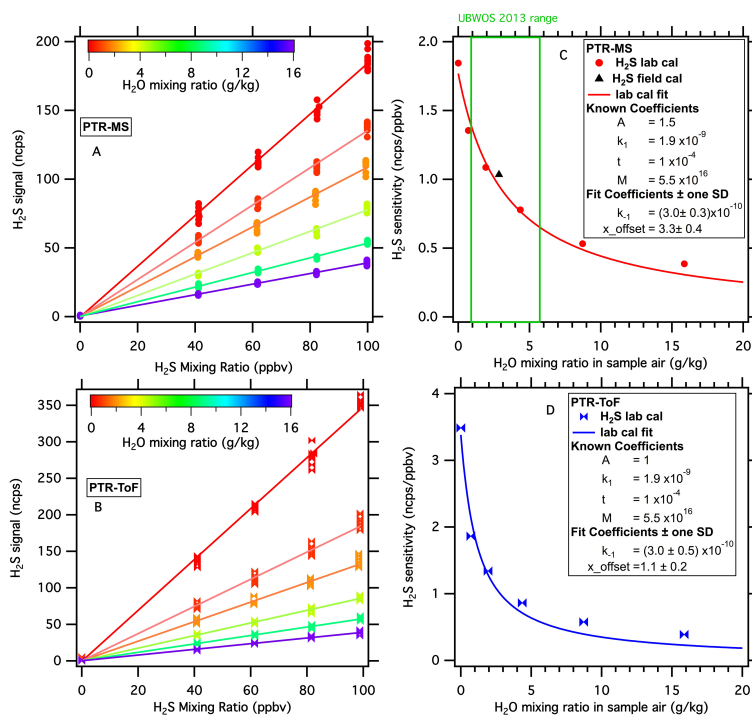


**Figure 4.** H<sub>2</sub>S laboratory calibration curves at different humidities (expressed in H<sub>2</sub>O mass mixing ratios) for (a) PTR-MS with an average H<sub>3</sub>O<sup>+</sup> ion signals of 25 million cps and (b) PTR-ToF-MS with an average H<sub>3</sub>O<sup>+</sup> of 8.8 million cps duty cycle corrected and 1.2 million cps actual counts. The sensitivity of (c) PTR-MS and (d) PTR-ToF-MS for H<sub>2</sub>S measurement dependent on humidity with the exponential fit of Eq. (6).

and  $0.06 \pm 0.006$  for the PTR-MS and PTR-ToF-MS, respectively. These are unrealistic values suggesting that the known coefficients that were used for the fit were not all appropriate. As mentioned earlier, the coefficients of  $k_1$  and  $k_{-1}$  obtained at 296 K may be different for the collision conditions in the drift tube. In fact, it is likely that they increase due to the elevated ion kinetic energy in the drift tube. Therefore, we re-fit the sensitivities by holding the transmission ratio  $A$  fixed with more reasonable values (1.5 and 1 for PTR-MS and PTR-ToF) and allowing  $k_{-1}$  as free parameters in the fit instead. As shown in Fig. 4c and d, the fit gives the same  $k_{-1}$  of  $(3.0 \pm 0.3) \times 10^{-10} \text{ cm}^3 \text{ molecule}^{-1} \text{ s}^{-1}$  for PTR-MS and  $(3.0 \pm 0.5) \times 10^{-10} \text{ cm}^3 \text{ molecule}^{-1} \text{ s}^{-1}$  for PTR-ToF, which are 2 orders of magnitude higher than the value obtained at ambient temperature ( $4.4 \times 10^{-12} \text{ cm}^3 \text{ molecule}^{-1} \text{ s}^{-1}$ ) (Tanaka et al., 1978). Such high values may also be unrealistic, so the most likely explanation may be a combination of uncertainties in the reaction rate coefficients as well as the mass transmission. The fit offsets of the water mixing ratio from ion source are  $3.3 \pm 0.4$  and  $1.1 \pm 0.2 \text{ g kg}^{-1}$  (corresponding to  $(86.9 \pm 10.4) \%$  and  $(29.1 \pm 5.2) \%$  RH at STP) for PTR-MS and PTR-ToF-MS, respectively. The exponential decay of the sensitivity from the laboratory calibration is well represented by the fit derived from the proton transfer reactions (R1a) and (R1b).

As shown in Fig. 4c, the water vapor mixing ratios ranged from 1 to  $6 \text{ g kg}^{-1}$  during UBWOS 2013, which gives H<sub>2</sub>S sensitivities ranging from  $0.6\text{--}1.4 \text{ ncps ppbv}^{-1}$  (and  $20\text{--}34 \text{ cps ppbv}^{-1}$ ) for PTR-MS and  $0.5\text{--}1.9 \text{ ncps ppbv}^{-1}$  (and  $1.0\text{--}2.2 \text{ cps ppbv}^{-1}$ ) for PTR-ToF-MS. This is much lower than for other VOCs, which typically have sensitivities ranging from 13.3 for methanol to  $31.3 \text{ ncps ppbv}^{-1}$  for acetone by PTR-MS (Warneke et al., 2011b). Figure 4c also shows a calibration conducted at the Horse Pool site during UBWOS 2013 (triangle point). A resulting sensitivity of  $1.03 \text{ ncps ppbv}^{-1}$  was determined under ambient conditions. This value agrees within 20 % with the laboratory calibration results.

The H<sub>2</sub>S detection limit by PTR-MS was determined from the laboratory calibration measurements at H<sub>2</sub>S VMR = 0. For the ambient humidity conditions during UBWOS 2013 ( $2.8 \text{ g kg}^{-1}$  on average), the H<sub>2</sub>S detection limit by PTR-MS is  $0.35 \text{ ppbv}$  (signal-to-noise = 3).

### 3.3 Ambient measurements and inter-comparison

Here we demonstrate how the H<sub>2</sub>S mixing ratios were determined from the ambient measurements by PTR-MS during a 4-day period between 29 January and 1 February 2013 at the Horse Pool site. This period was selected because it covered a wide range of humidities, H<sub>2</sub>S and methanol levels. As described earlier, because of the high levels ( $100 \text{ s ppbv}^{-1}$ ) of methanol from the gas and oil production in Uintah basin, there is interference in the H<sub>3</sub>S<sup>+</sup> signal from the methanol isotope containing oxygen isotope <sup>18</sup>O. In Fig. 5, the mea-

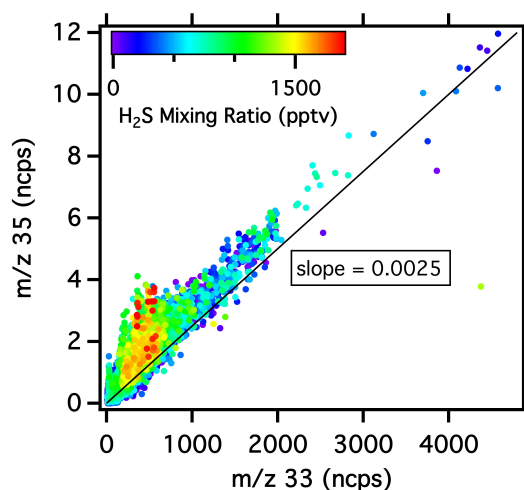


**Figure 5.** The relationship between  $m/z$  35 and  $m/z$  33 color-coded by the H<sub>2</sub>S mixing ratio measured by the CRDS instrument. The line with a slope of 0.0025 that is the <sup>18</sup>O natural abundance overlaps with the measurements at zero H<sub>2</sub>S mixing ratio levels (purple points).

sured signals at  $m/z$  35 are plotted against the methanol signals at  $m/z$  33 color-coded with H<sub>2</sub>S mixing ratios measured by the CRDS during UBWOS 2013. For the data with low H<sub>2</sub>S levels (purple-blue points), the signals at  $m/z$  35 show a linear relationship with the signals at  $m/z$  33. The linear slope,  $\sim 0.002$ , is equal to the natural abundance of the isotope <sup>18</sup>O in methanol (0.2 %) and indicates that the signal CH<sub>3</sub><sup>18</sup>OH is dominating  $m/z$  35. Of course there are also the <sup>14</sup>C (carbon), <sup>2</sup>D (deuterium) and <sup>3</sup>T (tritium) isotopes, but their abundance is much smaller so we will ignore those here to simplify the discussion. It is clear that much of the signal at  $m/z$  35 is from CH<sub>3</sub><sup>18</sup>OH. As the H<sub>2</sub>S mixing ratio increases (yellow-red points), the relationship between signals at  $m/z$  35 and  $m/z$  33 diverts from the line attributed to the CH<sub>3</sub><sup>18</sup>OH signal. In these cases, H<sub>2</sub>S is a significant contributor to the  $m/z$  35 signals. This shows that the H<sub>2</sub>S can be detected by PTR-MS at  $m/z$  35. At several hundred ppbv of methanol as often observed at Horse Pool, the signal at  $m/z$  35 was corrected for the contribution from CH<sub>3</sub><sup>18</sup>OH before the  $m/z$  35 signal is used to obtain H<sub>2</sub>S, which was calculated by subtracting the product of the methanol signal at  $m/z$  33 multiplied by the natural abundance of the isotope <sup>18</sup>O (0.2 %, Fig. 6a).

The ambient and background signals of  $m/z$  35 were normalized to the primary ion signal, as shown in Fig. 6a. The instrument background was measured by passing ambient flow through a catalytic converter, which removed H<sub>2</sub>S and methanol isotopologues, every 3 h 15 min for 153 s. The correlation between background signals of  $m/z$  35 and water vapor mixing ratio is very small ( $r^2 = 0.005$ ), indicating that the background data from the catalytic converter serves as a good zero for the H<sub>2</sub>S removal (background  $< 0.5 \text{ ncps}$ ).

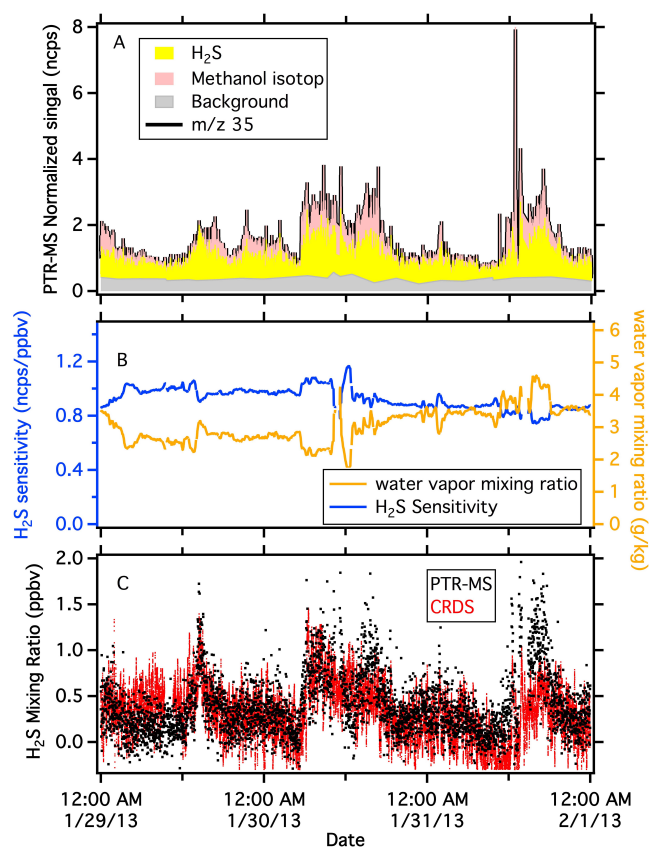


**Figure 6.** Time series of H<sub>2</sub>S measurements during UBWOS campaign 2013. (a) PTR-MS raw signals at  $m/z$  35 and the contributions from H<sub>2</sub>S, CH<sub>3</sub><sup>18</sup>OH and instrument background. (b) Calibration factor estimated from the water vapor mixing ratio by the fit in Fig. 4. (c) H<sub>2</sub>S mixing ratio comparison between the resulting PTR-MS and CRDS measurements. The signal from PTR-MS is 1 min average, and CRDS is an average of the last 5 min measurements over 5 s intervals.

However, it should be noted that at high H<sub>2</sub>S concentrations, the catalyst could deteriorate quickly. The H<sub>2</sub>S signal at  $m/z$  35 was determined by subtracting an interpolated background and CH<sub>3</sub><sup>18</sup>OH contribution from the ambient data. Figure 6a shows the ambient measurements with stacked individual contributions to  $m/z$  35 from H<sub>2</sub>S itself, CH<sub>3</sub><sup>18</sup>OH and the background. The associated uncertainties ( $1\sigma$  error) of the normalized signals were estimated from Poisson distribution of the raw counts at  $m/z$  35, which gives 25 % of the relative precision. The subtraction of CH<sub>3</sub><sup>18</sup>OH adds on average 5 % to the uncertainty of the H<sub>2</sub>S signals.

In Fig. 6b, the H<sub>2</sub>S sensitivity was determined from the water vapor mixing ratio using the exponential fit (Eq. 5) from the laboratory calibration given in Fig. 4c. The water vapor mixing ratio was calculated from the ratio of signals at  $m/z$  37 to  $m/z$  19 (de Gouw and Warneke, 2007; de Gouw et al., 2003a; Warneke et al., 2011b). H<sub>2</sub>S mixing ratios were calculated in Fig. 6c by dividing the normalized signals of

H<sub>2</sub>S (yellow section in Fig. 4a) by the sensitivity (blue line in Fig. 6b). The H<sub>2</sub>S measurement from a CRDS instrument is also shown in Fig. 6c. The measurements from both instruments show reasonable agreement during this short time period, confirming the potential of PTR-MS for accurate H<sub>2</sub>S measurements.

The time series of H<sub>2</sub>S mixing ratios at the Horse Pool site from the Picarro CRDS instrument and the PTR-ToF-MS together with the PTR-MS measurement during the whole UBWOS 2013 campaign are shown in Fig. 7a for inter-comparison purposes. All the data from these three instruments shown here are 5 min averages. The scatter plots of the PTR-MS data versus the CRDS data and versus the PTR-ToF-MS data are shown in Fig. 7c and c. The data in these graphs were fit with orthogonal distance regression (ODR fit, black lines) (Boggs et al., 1987; Press et al., 1991). The slope for the scatter plots of the PTR-MS versus CRDS is  $1.24 \pm 0.03$ . The  $R^2$  is 0.3 and this relatively low value is caused by the fact that both measurements are very close to their detection limits. The PTR-MS (uncertainty  $0.35 \text{ ppb} + 30\%$ ,  $3\sigma$  for 16 s integration) agrees with the CRDS data (uncertainty  $1 \text{ ppb} + 0.4\%$ ,  $1\sigma$ ) within the stated uncertainties. The negative values in the measurements from the CRDS instrument (Fig. 7a) indicate some drift issues although the data had been corrected based on the field calibration (on 4 February 2013), which may have limited the agreement between the two instruments.

For the PTR-ToF-MS data, the high resolution time-of-flight MS provides more detailed mass information for the H<sub>2</sub>S measurement. Figure 8 illustrates an example of the mass spectra and individual contribution from different species to the ambient raw measurements at  $m/z$  33, 34 and 35. The peak fits at different masses to the raw measurements provide quantitative ion counts for each trace. In Fig. 8a two peaks have been resolved at  $m/z$  33. As expected, the methanol signal dominates the measurement at  $m/z$  33. However, another minor peak is also clearly present at this mass. The peak fit result shows this minor peak is contributed by two different ions, whose mass difference is too small to be separated by ToF-MS. The O<sub>2</sub><sup>+</sup> ion with <sup>17</sup>O isotope has a mass of  $m/z$  32 9935 and HO<sub>2</sub><sup>+</sup> of  $m/z$  32 9971. In quadrupole MS, the interference on methanol measurements at  $m/z$  33 from <sup>16</sup>O<sup>17</sup>O<sup>+</sup> and HO<sub>2</sub><sup>+</sup> has been corrected by subtracting the background measurement, which includes both these impurities. Figure 8b shows the signals at  $m/z$  34 attributed from O<sub>2</sub><sup>+</sup> with <sup>18</sup>O isotope. Because this was the first deployment of continuous sampling by this PTR-ToF-MS for over a month right after delivery from the manufacturer, no instrument optimization was conducted before the UBWOS campaign. The O<sub>2</sub><sup>+</sup> and HO<sub>2</sub><sup>+</sup> signals were over a factor of 2 higher than in other PTR instruments under normal operation. The impurity ions O<sub>2</sub><sup>+</sup> formed from the air back streaming in the ion sources and can be reduced by tuning the voltages on the intermediate chamber between ion

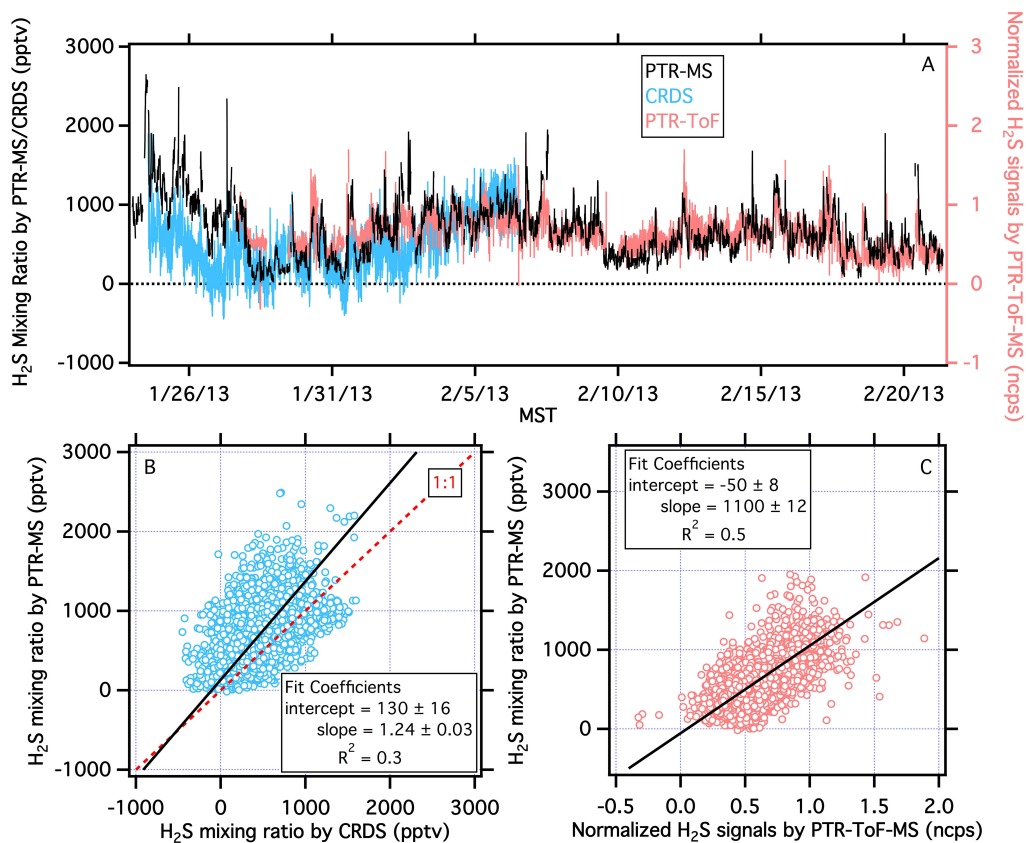


**Figure 7.** (a) Inter-comparison of H<sub>2</sub>S measurements from PTR-MS, PTR-ToF-MS and CRDS during UBWOS 2013 at Horse Pool ground site. All the measurements are 5 min averaged. The PTR-MS and CRDS measurements are plotted in mixing ratio on the left axis. PTR-ToF-MS measurements are in normalized counts per second (ncps) on the right axis. (b) Scatter plot of H<sub>2</sub>S measurements by PTR-MS vs. by CRDS. (c) Scatter plot of H<sub>2</sub>S measurements by PTR-MS vs. by PTR-ToF-MS.

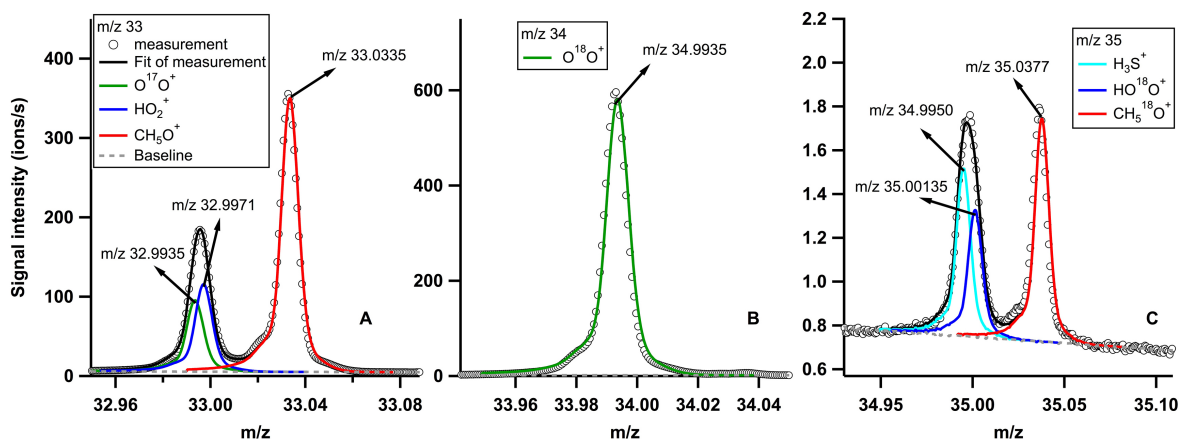


**Figure 8.** A common example of the mass spectra and peak fit for different species at  $m/z$  33, 34 and 35 from the measurements of PTR-ToF-MS. (a) Two peaks are shown in the raw measurements at  $m/z$  33. The first peak is contributed by both O<sub>2</sub><sup>+</sup> with <sup>17</sup>O isotope and HO<sub>2</sub><sup>+</sup>. The second peak is by methanol. (b) The signals at  $m/z$  34 are from O<sub>2</sub><sup>+</sup> with <sup>18</sup>O isotope. (c) There are two peaks in the raw measurements at  $m/z$  35. The first peak is contributed by a sum of H<sub>3</sub>S<sup>+</sup> (protonated H<sub>2</sub>S signal) and HO<sub>2</sub><sup>+</sup> with <sup>18</sup>O isotope. The second peak is from methanol with <sup>18</sup>O isotope.

source and drift tube. HO<sub>2</sub><sup>+</sup> is likely generated by endothermic proton transfer during ion extraction at the end of drift tube and this interference can be reduced by optimizing those voltage settings. The high level of these ions interferes with the H<sub>2</sub>S measurements. As shown in Fig. 8c, there were two peaks in the raw measurements at  $m/z$  35. The first peak is contributed by the sum of H<sub>3</sub>S<sup>+</sup> (protonated H<sub>2</sub>S signal) and HO<sub>2</sub><sup>+</sup> with <sup>18</sup>O isotope. The second peak is from methanol with <sup>18</sup>O isotope. The mixing ratio of H<sub>2</sub>S may still be extracted from the data after subtraction of the HO<sup>18</sup>O<sup>+</sup> signal, although the quality of the H<sub>2</sub>S data will clearly suffer from the overlap in peaks. In addition, the catalytic converter used with the PTR-ToF was not 100% efficient in removing H<sub>2</sub>S and determining the system background. For both these reasons, the H<sub>2</sub>S signal derived from the PTR-ToF has not been converted to a volume mixing ratio, but can still be compared semi-quantitatively with the PTR-MS. The diurnal and daily variation in H<sub>2</sub>S signals through the whole campaign are still present despite the absence of zeros. The time series of normalized H<sub>2</sub>S signals with HO<sup>18</sup>O<sup>+</sup> correction by PTR-ToF-MS is shown in Fig. 7a on the right axis. Despite the limitations to the PTR-ToF data, the normalized signals show many of the same features as observed by PTR-MS. Figure 7c shows the scatter plot of H<sub>2</sub>S mixing ratios measured by PTR-MS against the normalized signals by PTR-ToF-MS. The  $R^2$  for the comparison with PTR-MS is 0.5.

The comparison between these instruments gives more confidence in making reliable measurements of H<sub>2</sub>S and other VOCs by PTR-MS instruments. It should be noted that the PTR-MS we were using was not specifically optimized for the detection of H<sub>2</sub>S. However, there is potential to make better measurements if PTR-MS instrument settings were tuned to focus on H<sub>2</sub>S measurements with less uncertainty or higher sensitivity. For example, removing ambient water vapor before PTR-MS, increasing the dwell times and adjusting drift tube pressure and voltage would improve the H<sub>2</sub>S detection sensitivity. Also, for optimal H<sub>2</sub>S measurements, a catalyst that removes sulfur compounds more reliably is needed. On the other hand, controlling the humidity in the drift tube at a relatively high value would reduce the variability in the sensitivity, and thus improve the precision in the measurements.

### 3.4 Emission sources for H<sub>2</sub>S

As shown in the NOAA ESRL Mobile Laboratory measurement with ULW-PTR-MS (Fig. 3), the ambient mixing ratio of H<sub>2</sub>S was not uniformly distributed over the gas and oil field. Significant enhancements were observed at some locations downwind of production operations, e.g., evaporation ponds, and some separation and condensation tanks (e.g., drive on 27 February 2012, Fig. 3d). No calibrations for H<sub>2</sub>S were made for the ULW-PTR-MS instrument during UBWOS 2012. The calibration factors for other VOCs between the ULW-PTR-MS and PTR-MS instruments are

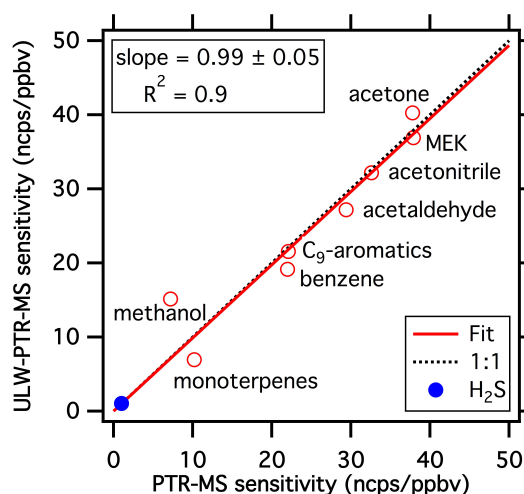


**Figure 9.** The estimate of ULW-PTR-MS calibration factor for H<sub>2</sub>S (blue triangle) from PTR-MS calibration at the field site during the UBWOS 2013, based on the comparison of calibration results for other compounds between the two PTR-MS instruments (red fit line). The calibration factors shown here are average of calibrations performed during the campaign.

shown in Fig. 9. A linear fit was used to describe the sensitivity comparison, showing a slope of  $0.99 \pm 0.05$ . Despite their different instrument settings, the sensitivities of the two instruments for a wide range of compounds agree well within their uncertainties (accuracy 30%). Thus, the calibration factor for H<sub>2</sub>S of the ULW-PTR-MS can be derived using that of the PTR-MS. Using the laboratory determined PTR-MS H<sub>2</sub>S calibration factor ( $1.04 \text{ ncps ppbv}^{-1}$  at ambient conditions), the estimated H<sub>2</sub>S calibration factor of ULW-PTR-MS from the fit was  $1.03 \pm 0.05 \text{ ncps ppbv}^{-1}$  (blue dot in Fig. 9).

The effect of humidity needs to be considered when applying the derived H<sub>2</sub>S calibration factor for the ULW-PTR-MS. During the ULW-PTR-MS measurements, the humidity conditions were similar to those for the H<sub>2</sub>S calibrations, indicating the estimated calibration factor is a reasonable approximation. The H<sub>2</sub>S mixing ratio of mobile measurements was determined with the same procedures as described for the stationary PTR-MS. The maximum H<sub>2</sub>S mixing ratios of  $9 \pm 4 \text{ ppmv}$  was observed at one location, downwind of a truck loading liquid condensate.

Figure 10 shows the time series of the H<sub>2</sub>S measurements by PTR-MS and methane measurements by the Picarro CRDS instrument during UBWOS 2013 at the Horse Pool site. The H<sub>2</sub>S mixing ratios show a good correlation with methane throughout the whole campaign. A scatter plot for the comparison between H<sub>2</sub>S and methane is shown in Fig. 11. An orthogonal distance regression fit with fixed intercept on  $x$  axis as methane background ( $1.85 \text{ ppmv}$ ) is used to calculate an enhancement ratio,  $\Delta\text{H}_2\text{S}/\Delta\text{CH}_4$ . An overall enhancement ratio of  $0.11 \text{ ppbv ppmv}^{-1}$  (solid line) for  $\Delta\text{H}_2\text{S}/\Delta\text{CH}_4$  was found in the Uintah Basin. The

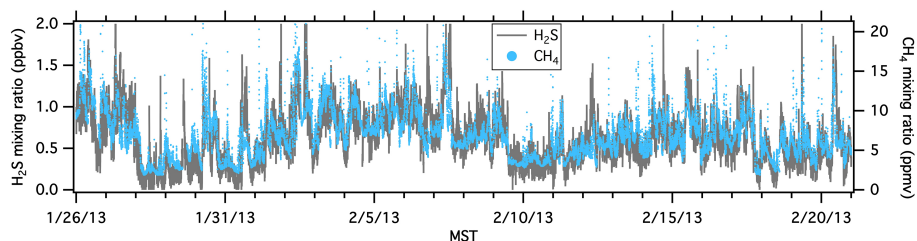


**Figure 10.** Time series of H<sub>2</sub>S measurements by PTR-MS and CH<sub>4</sub> mixing ratios by CRDS during UBWOS 2013 at Horse Pool ground site.

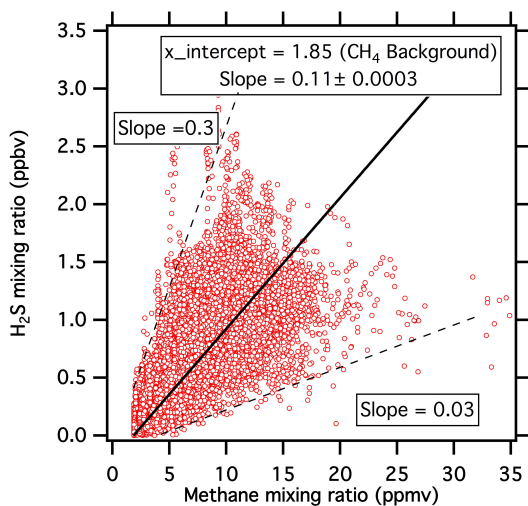


**Figure 11.** Scatter plot of H<sub>2</sub>S mixing ratio measured by PTR-MS vs. methane measured by CRDS with linear fit to the data shown in Fig. 10. The slope values are in units of ppbv ppmv<sup>-1</sup>. The dashed lines represent the maximum and minimum enhancement ratios.

correlation between H<sub>2</sub>S and CH<sub>4</sub> suggests that H<sub>2</sub>S was released with CH<sub>4</sub> and other VOCs from oil and gas operations on a routine basis, resulting in elevated background levels, rather than just from a few isolated sources as the results from the surveys suggested (Fig. 3). Whereas the very high H<sub>2</sub>S emissions observed downwind of some individual oil and gas wells can lead to short-term high levels close to point sources, these may be less important H<sub>2</sub>S sources averaged over the basin. An average H<sub>2</sub>S mixing ratio of  $0.6 \pm 0.3$  ppbv was observed at the Horse Pool ground site in 2013. The remaining scatter in Fig. 11 may be influenced by the fact that  $\Delta\text{H}_2\text{S}/\Delta\text{CH}_4$  are not necessarily the same for all gas and oil wells. H<sub>2</sub>S production mechanisms (Environmental Protection Agency et al., 1993) are different for each well. H<sub>2</sub>S production and subsequent emission can vary depending on the activity of anaerobic bacteria and the distribution and availability of sulfates and sulfur-containing organic compounds in the well. The data suggest that the ratio varied within a factor of 10 ( $0.03\text{--}0.3$  ppbv ppmv<sup>-1</sup>, Fig. 11). The  $\Delta\text{H}_2\text{S}/\Delta\text{CH}_4$  enhancement ratio of  $0.11$  ppbv ppmv<sup>-1</sup> is equivalent to  $\sim 100$  ppmv H<sub>2</sub>S in natural gas, assuming

that methane is on average 90 % of natural gas. This is much larger than the threshold of 4 ppmv under standard temperature and pressure, above which natural gas is defined as sour (Natural Gas.Org, 2011). In contrast, the natural gas in Uintah basin is not considered to be sour, i.e. gas sweetening is typically not required. This combined findings suggest that the atmospheric emissions are enriched in H<sub>2</sub>S relative to the raw gas. It is not known in which exact industrial process this enrichment occurs.

Using the average  $\Delta\text{H}_2\text{S}/\Delta\text{CH}_4$  ratio determined here, we estimated the total H<sub>2</sub>S emissions in the basin. This is done using the methane emission measurements from Karion et al. (2013), who estimated a total average release of  $(55 \pm 15) \times 10^3$  kg h<sup>-1</sup> using aircraft measurements in February 2012. Assuming similar emissions in 2013, we estimate the total emissions of H<sub>2</sub>S in the Uintah basin to be  $6.1 \pm 1.7$  kg h<sup>-1</sup>, or  $(5.3 \pm 1.5) \times 10^{-5}$  Tg a<sup>-1</sup>. The total source of H<sub>2</sub>S to the atmosphere is highly uncertain (Kourtidis et al., 2004; Watts, 2000). One study estimates the global anthropogenic source as 3.3 Tg a<sup>-1</sup> and the total source as 7.7 Tg a<sup>-1</sup> (Möller, 1984; Watts, 2000). Another study puts the global terrestrial source at the much smaller number of 0.075 Tg a<sup>-1</sup> (Bates et al., 1992).

#### 4 Conclusions

In this paper we demonstrate fast time response measurements of H<sub>2</sub>S using three different PTR-MS instruments that were operated at standard instrument settings for various VOCs detection in the Uintah Basin with oil and gas producing wells during two wintertime field studies in 2012 and 2013. Mobile laboratory measurements were made possible using a compact and lightweight ULW-PTR-MS during UBWOS 2012. The ULW-PTR-MS was not calibrated but showed varying levels of H<sub>2</sub>S across the field and provided evidence for the existence of multiple point sources in oil and gas field, which prompted more work to explore the performance of PTR instruments for H<sub>2</sub>S. During UBWOS 2013, H<sub>2</sub>S was measured by the PTR-MS together with the PTR-ToF-MS for inter-comparison purposes. A specific calibration study for H<sub>2</sub>S was undertaken for these field measurements. The humidity dependence of H<sub>2</sub>S detection by PTR-MS was determined in the laboratory and agreed within

20 % with the calibration determined in the field for the PTR-MS instrument. The observed sensitivities at various humidities appear to be explained by kinetics when we allow for a higher backward reaction rate and an offset in water vapor concentration in the drift tube. The PTR-MS H<sub>2</sub>S sensitivity was determined to be 0.6–1.4 ncps ppbv<sup>-1</sup> during during UBWOS 2013, about 3–10 % of the sensitivity to most other compounds detected by PTR-MS. This is due to the proton affinity of H<sub>2</sub>S that is only slightly higher than that of water, leading to a non-negligible backward proton transfer reaction. Inter-comparison of H<sub>2</sub>S measurements shows the PTR-MS as a valid method for the measurement of H<sub>2</sub>S. On average 4 ± 2 ppbv H<sub>2</sub>S was observed from the NOAA ESRL Mobile Laboratory close to well pads during UBWOS 2012 and 0.6 ± 0.3 ppbv H<sub>2</sub>S at the Horse Pool site during UBWOS 2013 in the Uintah Basin, most likely due to routine emissions from oil and gas facilities, which was supported by evidence of the correlation between H<sub>2</sub>S and CH<sub>4</sub>. Significant H<sub>2</sub>S mixing ratios up to 9 ± 4 ppmv from a condensation tank being serviced were observed during the mobile measurements. This study suggests that H<sub>2</sub>S emissions associated with oil and gas production can lead to short-term high levels close to point sources, and elevated background levels away from those sources. This study shows PTR-MS is able to make reliable measurements of H<sub>2</sub>S down to levels of 350 pptv. Potentially better measurements are possible if the PTR instrument settings were optimized for H<sub>2</sub>S.

*Acknowledgements.* We thank Russ Schnell, Jonathan Kofler, Steve Brown, Pete Edwards and Bill Dube for their contributions to this work. R. Li's work was supported by the CIRES Innovative Research Program. The use of PTR-ToF-MS and Picarro CRDS (CH<sub>4</sub>/H<sub>2</sub>S) was supported by NSF. The 2012 and 2013 UBWOS campaigns were made possible by support from the following organizations: State of Utah, US Environmental Protection Agency, Western Energy Alliance, Uinta Impact Mitigation Special Service District, and the Bureau of Land Management. The scientific results and conclusions, as well as any views or opinions expressed herein, are those of the author(s) and do not necessarily reflect the views of the Uinta Basin Winter Ozone and Air Quality Study collaborators or funding agencies.

Edited by: P. B. Shepson

## References

- Bandy, A. R., Tucker, B. J., and Maroulis, P. J.: Determination of part-per-trillion by volume levels of atmospheric carbon disulfide by gas-chromatography mass-spectrometry, *Anal. Chem.*, 57, 1310–1314, 1985.
- Bates, T. S., Lamb, B. K., Guenther, A., Dignon, J., and Stoiber, R. E.: Sulfur emissions to the atmosphere from natural sources, *J. Atmos. Chem.*, 14, 315–337, 1992.
- Beauchamp, J., Frasnelli, J., Buettner, A., Scheibe, M., Hansel, A., and Hummel, T.: Characterization of an olfactometer by proton-

- transfer-reaction mass spectrometry, *Meas. Sci. Technol.*, 21, 025801, doi:10.1088/0957-0233/21/2/025801, 2010.
- Benner, R. L. and Stedman, D. H.: Universal sulfur detection by chemiluminescence, *Anal. Chem.*, 61, 1268–1271, 1989.
- Benner, R. L. and Stedman, D. H.: Field evaluation of the sulfur chemiluminescence detector, *Environ. Sci. Technol.*, 24, 1592–1596, 1990.
- Boggs, P. T., Byrd, R. H., and Schnabel, R. B.: A stable and efficient algorithm for nonlinear orthogonal distance regression, *SIAM J. Sci. Stat. Comp.*, 8, 1052–1078, 1987.
- Chen, H., Winderlich, J., Gerbig, C., Hofer, A., Rella, C. W., Crosson, E. R., Van Pelt, A. D., Steinbach, J., Kolle, O., Beck, V., Daube, B. C., Gottlieb, E. W., Chow, V. Y., Santoni, G. W., and Wofsy, S. C.: High-accuracy continuous airborne measurements of greenhouse gases (CO<sub>2</sub> and CH<sub>4</sub>) using the cavity ring-down spectroscopy (CRDS) technique, *Atmos. Meas. Tech.*, 3, 375–386, doi:10.5194/amt-3-375-2010, 2010.
- Chou, S., Fay, M., Keith, S., Ingerman, L., and Chappell, L.: Toxicological Profile For Hydrogen Sulfide Services, U.S. Department of Health and Human Services, Public Health Service, Agency for Toxic Substances and Disease Registry, 2006.
- de Gouw, J. and Warneke, C.: Measurements of volatile organic compounds in the earth's atmosphere using proton-transfer-reaction mass spectrometry, *Mass Spectrom. Rev.*, 26, 223–257, 2007.
- de Gouw, J., Warneke, C., Karl, T., Eerdekens, G., van der Veen, C., and Fall, R.: Sensitivity and specificity of atmospheric trace gas detection by proton-transfer-reaction mass spectrometry, *Int. J. Mass Spectrom.*, 223–224, 365–382, 2003a.
- de Gouw, J. A., Goldan, P. D., Warneke, C., Kuster, W. C., Roberts, J. M., Marchewka, M., Bertman, S. B., Pszenny, A. A. P., and Keene, W. C.: Validation of proton transfer reaction-mass spectrometry (PTR-MS) measurements of gas-phase organic compounds in the atmosphere during the New England Air Quality Study (NEAQS) in 2002, *J. Geophys. Res.*, 108, 4682, 2003b.
- Dubyk, S., Mustafa, S., and Graham, A.: Trip Report: H<sub>2</sub>S Survey, 18–22 March, 2002.
- Environmental Protection Agency, E., Office of Air Quality Planning Standards, and Office of Solid Waste Emergency Response: Report to Congress on Hydrogen Sulfide Air Emissions Associated with the Extraction of Oil and Natural Gas, 1993.
- Feilberg, A., Liu, D., Adamsen, A. P. S., Hansen, M. J., and Jonassen, K. E. N.: Odorant Emissions from Intensive Pig Production Measured by Online Proton-Transfer-Reaction Mass Spectrometry, *Environ. Sci. Technol.*, 44, 5894–5900, 2010.
- Feilberg, A., Liu, D., and Hansen, M. J.: Measurement of H<sub>2</sub>S by PTR-MS: Experiences and Implications, *Innsbruck*, 98–101, 2013.
- Graus, M., Müller, M., and Hansel, A.: High Resolution PTR-TOF: Quantification and Formula Confirmation of VOC in Real Time, *J. Am. Soc. Mass Spectrom.*, 21, 1037–1044, 2010.
- Heber, A. J., Casey, K. D., Caramanica, A. P., Mickey, K. J., and Cortus, E. L.: Emissions data from two sow barns and one swine farrowing room in Oklahoma Agency, National Air Emissions Monitoring Study, EPA website, 2010.
- Hunter, E. P. L. and Lias, S. G.: Evaluated Gas Phase Basicities and Proton Affinities of Molecules: An Update, *J. Phys. Chem. Ref. Data*, 27, 413–656, 1998.

- Inomata, S., Tanimoto, H., Kameyama, S., Tsunogai, U., Irie, H., Kanaya, Y., and Wang, Z.: Technical Note: Determination of formaldehyde mixing ratios in air with PTR-MS: laboratory experiments and field measurements, *Atmos. Chem. Phys.*, 8, 273–284, doi:10.5194/acp-8-273-2008, 2008.
- Karion, A., Sweeney, C., Petron, G., Frost, G., Hardesty, R. M., Kofler, J., Miller, B. R., Newberger, T., Wolter, S., Banta, R., Brewer, A., Dlugokencky, E., Lang, P., Montzka, S. A., Schnell, R., Tans, P., Trainer, M., Zamora, R., and Conley, S.: Methane emissions estimate from airborne measurements over a western United States natural gas field, *Geophys. Res. Lett.*, 40, 4393–4397, 2013.
- Kelly, T. J., Gaffney, J. S., Phillips, M. F., and Tanner, R. L.: Chemiluminescent detection of reduced sulfur compounds with ozone, *Anal. Chem.*, 55, 135–138, 1983.
- Khan, M. A. H., Whelan, M. E., and Rhew, R. C.: Analysis of low concentration reduced sulfur compounds (RSCs) in air: Storage issues and measurement by gas chromatography with sulfur chemiluminescence detection, *Talanta*, 88, 581–586, 2012.
- Knighton, W. B., Fortner, E. C., Midey, A. J., Viggiano, A. A., Haddon, S. C., Wood, E. C., and Kolb, C. E.: HCN detection with a proton transfer reaction mass spectrometer, *Int. J. Mass Spectrom.*, 283, 112–121, 2009.
- Kourtidis, K., Kelesis, A., Maggana, M., and Petrakakis, M.: Substantial traffic emissions contribution to the global H<sub>2</sub>S budget, *Geophys. Res. Lett.*, 31, L18107, doi:10.1029/2004GL020713, 2004.
- Layfon, D. W. and Cederwall, R. T.: Predicting and Managing the Health Risks of Sour-Gas Wells, *JAPCA*, 37, 1185–1190, 1987.
- Liu, D., Feilberg, A., Adamsen, A. P. S., and Jonassen, K. E. N.: The effect of slurry treatment including ozonation on odorant reduction measured by in-situ PTR-MS, *Atmos. Environ.*, 45, 3786–3793, 2011.
- Liu, D., Pedresen, C. L., Nielsen, L. P., and Feilberg, A.: PTR-MS application for biofiltration kinetics assessment of odour removal, 6th International Conference on Proton Transfer Reaction Mass Spectrometry and its Applications, 2013.
- Liu, Z., Powers, W., Karcher, D., Angel, R., and Applegate, T. J.: Effect of amino acid formulation and supplementation on air emissions from tom turkeys, *American Society of Agricultural and Biological Engineers, Transactions*, 54, 617–628, 2011.
- Martin, R., Moore, K., Mansfield, M., Hill, S., Harper, K., and Shorthill, H.: Final report: Uinta Basin winter ozone and air quality study December 2010–March 2011, Energy Dynamics Laboratory, EDL/11-039, 2011.
- Möller, D.: Estimation of the global man-made sulphur emission, *Atmos. Environ.*, 18, 19–27, 1984.
- Müller, M., Mikoviny, T., Jud, W., D’Anna, B., and Wisthaler, A.: A new software tool for the analysis of high resolution PTR-TOF mass spectra, *Chemometr. Intell. Lab.*, 127, 158–165, 2013.
- Natural Gas.Org: <http://naturalgas.org/naturalgas/processing-ng/> (last access: 10 February 2014), 2011.
- Office of Geological Survey, Department of Geological Survey: [http://www.michigan.gov/deq/0,4561,7-135-3311\\_4111\\_4231-9162--,00.html](http://www.michigan.gov/deq/0,4561,7-135-3311_4111_4231-9162--,00.html) (last access: 23 January 2014), 2013.
- Press, W. H., Flannery, B., Teukolsky, S., and Vetterling, W.: Numerical recipes in C, 1988, Cambridge: Cambridge University-Press, 222 pp., 1991.
- Saha, C. K., Feilberg, A., Zhang, G. Q., and Adamsen, A. P. S.: Effects of airflow on odorants’ emissions in a model pig house – A laboratory study using Proton-Transfer-Reaction Mass Spectrometry (PTR-MS), *Sci. Total Environ.*, 410, 161–171, 2011.
- Skrtic, L.: Hydrogen sulfide, oil & gas, and people’s health, Master’s of Science, Energy and Resources Group, University of California, Berkeley, 2006.
- Spurlin, S. R. and Yeung, E. S.: On-line chemiluminescence detector for hydrogen sulfide and methyl mercaptan, *Anal. Chem.*, 54, 318–320, 1982.
- Stuedler, P. A. and Kijowski, W.: Determination of reduced sulfur gases in air by solid adsorbent preconcentration and gas chromatography, *Anal. Chem.*, 56, 1432–1436, 1984.
- Tanaka, K., Mackay, G. I., and Bohme, D. K.: Rate and equilibrium constant measurements for gas-phase proton-transfer reactions involving H<sub>2</sub>O, H<sub>2</sub>S, HCN, and H<sub>2</sub>CO, *Can. J. Chemistry*, 56, 193–204, 1978.
- Tarver, G. A. and Dasgupta, P. K.: Oil Field Hydrogen Sulfide in Texas: Emission Estimates and Fate, *Environ. Sci. Technol.*, 31, 3669–3676, 1997.
- Vlasenko, A., Macdonald, A. M., Sjostedt, S. J., and Abbatt, J. P. D.: Formaldehyde measurements by Proton transfer reaction – Mass Spectrometry (PTR-MS): correction for humidity effects, *Atmos. Meas. Tech.*, 3, 1055–1062, doi:10.5194/amt-3-1055-2010, 2010.
- Warneke, C., van der Veen, C., Luxembourg, S., de Gouw, J. A., and Kok, A.: Measurements of benzene and toluene in ambient air using proton-transfer-reaction mass spectrometry: calibration, humidity dependence, and field intercomparison, *Int. J. Mass Spectrom.*, 207, 167–182, 2001.
- Warneke, C., de Gouw, J. A., Kuster, W. C., Goldan, P. D., and Fall, R.: Validation of Atmospheric VOC Measurements by Proton-Transfer- Reaction Mass Spectrometry Using a Gas-Chromatographic Preseparation Method, *Environ. Sci. Technol.*, 37, 2494–2501, 2003.
- Warneke, C., Roberts, J. M., Veres, P., Gilman, J., Kuster, W. C., Burling, I., Yokelson, R., and de Gouw, J. A.: VOC identification and inter-comparison from laboratory biomass burning using PTR-MS and PIT-MS, *Int. J. Mass Spectrom.*, 303, 6–14, 2011a.
- Warneke, C., Veres, P., Holloway, J. S., Stutz, J., Tsai, C., Alvarez, S., Rappenglueck, B., Fehsenfeld, F. C., Graus, M., Gilman, J. B., and de Gouw, J. A.: Airborne formaldehyde measurements using PTR-MS: calibration, humidity dependence, inter-comparison and initial results, *Atmos. Meas. Tech.*, 4, 2345–2358, doi:10.5194/amt-4-2345-2011, 2011b.
- Warneke, C., Geiger, F., Edwards, P. M., Dube, W., Pétron, G., Kofler, J., Zahn, A., Brown, S. S., Graus, M., Gilman, J. B., Lerner, B. M., Peischl, J., Ryerson, T. B., de Gouw, J. A., and Roberts, J. M.: Volatile organic compound emissions from the oil and natural gas industry in the Uintah Basin, Utah: oil and gas well pad emissions compared to ambient air composition, *Atmos. Chem. Phys.*, 14, 10977–10988, doi:10.5194/acp-14-10977-2014, 2014.
- Watts, S. F.: The mass budgets of carbonyl sulfide, dimethyl sulfide, carbon disulfide and hydrogen sulfide – phytoplankton production in the surface ocean, *Atmos. Environ.*, 34, 761–779, 2000.